

## Kondo effect in double quantum dots with interdot repulsion

J. Mravlje,<sup>1</sup> A. Ramšak,<sup>2,1</sup> and T. Rejec<sup>1,2,3</sup>

<sup>1</sup>Jožef Stefan Institute, Ljubljana, Slovenia

<sup>2</sup>Faculty of Mathematics and Physics, University of Ljubljana, Slovenia

<sup>3</sup>Department of Physics, Ben-Gurion University, Beer-Sheva, Israel

(Received 7 March 2006; published 9 June 2006)

We investigate a symmetrical double quantum dot system serially attached to the leads. The emphasis is on the numerical analysis of finite interdot tunneling in the presence of interdot repulsive capacitive coupling. The results reveal the competition between extended Kondo phases and local singlet phases in spin and charge degrees of freedom. The corresponding phase diagram is determined quantitatively.

DOI: 10.1103/PhysRevB.73.241305

PACS number(s): 73.23.-b, 73.63.Kv, 72.15.Qm

Quantum dots<sup>1-4</sup> provide, in addition to various applications in proposed spintronics<sup>5</sup> and quantum computation<sup>6,7</sup> devices, a playground for studying phenomena known in bulk condensed-matter systems. Specifically, the Kondo effect was found to play an important role in single<sup>8</sup> and double quantum dot<sup>9-11</sup> (DQD) systems. From early theoretical work on the low-temperature properties of the two-impurity Kondo Hamiltonian<sup>13,14</sup> it is known that either localized moments each form its own Kondo singlet with delocalized electrons in the leads—*double Kondo* (2K) phase—or they form a *local spin-singlet* (LSS) state decoupled from delocalized electrons. The crossover between the two regimes is the consequence of competing energies of the Kondo singlet with Kondo temperature  $T_K$  and of LSS formation  $J$ . Similar results were obtained by the analysis of a two-impurity Anderson model by means of the slave-boson formalism<sup>15-19</sup> and numerical renormalization group (NRG).<sup>20,21</sup> Similar behavior was also found in particular regimes of a triple quantum dot system.<sup>22</sup>

Here we focus on the role the interdot (capacitive) interaction plays in the electron transport through serially coupled DQDs. The influence of the capacitive coupling was already studied by means of the equation-of-motion method,<sup>23-26</sup> which, however, fails to capture the Kondo correlations accurately. On the other hand, the Kondo correlations were considered in the limit of vanishing tunnel coupling and strong interdot interaction where the ground state of the isolated DQD exhibits fourfold degeneracy: in addition to spin degeneracy, singly occupied states labeled with (1,0) and (0,1) are also degenerate, leading to orbital Kondo behavior.<sup>27-31</sup> Here  $(n_1, n_2)$  corresponds to occupancies  $n_1$  and  $n_2$  of the two dots. The simultaneous presence of spin and orbital degeneracy results in enhanced Kondo temperature  $T_K(N) \sim \sqrt{J' \rho_0 N} \exp(-1/J' \rho_0 N)$ , where  $N$  is the degeneracy,  $\rho_0$  the noninteracting density of states, and  $J'$  the corresponding Schrieffer-Wolf prefactor.<sup>28</sup> The isospin Kondo resonance was observed indirectly in the measurements of enhanced conductance through DQDs,<sup>9-12</sup> and carbon nanotubes,<sup>32,33</sup> and also directly, in the bulk, with the techniques of scanning tunneling microscopy.<sup>34</sup> Recently the *enhanced Kondo temperature* (EKT) phase was predicted for DQDs with interdot interaction  $V=U$  in the absence of tunneling between the dots also at half filling,<sup>35</sup> i.e.,  $n=n_1+n_2=2$ . The main characteristics of this phase at low tempera-

tures is the enhanced width of the Kondo resonance (i.e., Kondo temperature  $T_K$ ) on top of an incoherent continuum in the density of states. However, the analysis of capacitively coupled DQDs with finite interdot tunneling rates has been lacking to date and we address this issue in the present paper.

We model the DQD shown in the inset of Fig. 1(c) by the Anderson-type Hamiltonian  $H=H_d+H_1$ , where  $H_d$  corresponds to the isolated dots,

$$H_d = \sum_{i=1,2} (\epsilon n_i + U n_{i\uparrow} n_{i\downarrow}) + V n_1 n_2 - t \sum_{\sigma} (c_{1\sigma}^{\dagger} c_{2\sigma} + \text{H.c.}),$$

with  $n_i = n_{i\uparrow} + n_{i\downarrow}$ ,  $n_{i\sigma} = c_{i\sigma}^{\dagger} c_{i\sigma}$ . The dots are coupled by a tunneling matrix element  $t$  and a capacitive  $V$  term. The on-site energies  $\epsilon$  and the Hubbard repulsion  $U$  are taken equal for both dots.  $H_1$  corresponds to the noninteracting left and right tight-binding leads and to the coupling of the DQD to the leads,

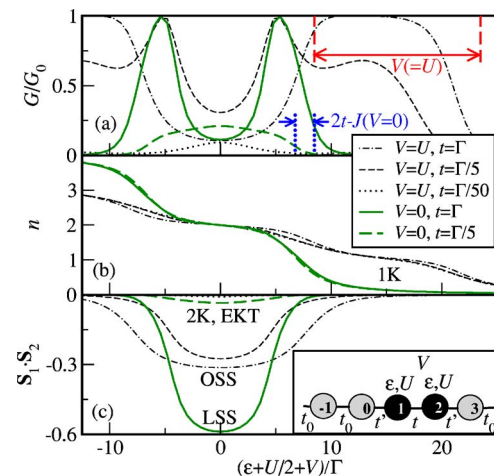


FIG. 1. (Color online) Conductance (a), occupancy (b), and spin-spin correlation (c) of a DQD for  $V=0$  (thick) and  $U$  (thin). The vertical lines for  $V=U$  (dashed) and 0 (dotted) correspond to transitions of an isolated DQD between  $n=0$ ,  $n=1$  and  $n=1$ ,  $n=2$  for  $t=\Gamma$ . Spin-singlet regimes (LSS, OSS) and Kondo regimes (2K, EKT, 1K) are indicated with labels. Inset: DQD system with both inter- and intradot Coulomb coupling, attached to noninteracting leads.

$$H_1 = -t_0 \sum_{i \neq 0,1,2} c_{i\sigma}^\dagger c_{i+1\sigma} - t' \sum_{\sigma} (c_{0\sigma}^\dagger c_{1\sigma} + c_{3\sigma}^\dagger c_{2\sigma}) + \text{H.c.},$$

where the sites are labeled as shown in the inset of Fig. 1(c).

In this Rapid Communication we study the low-temperature properties of the DQD, derived from the ground state at  $T=0$ , determined by the Gunnarsson and Schönhammer projection-operator method.<sup>36,37</sup> The conductance is calculated using the sine formula<sup>37</sup>  $G = G_0 \sin^2[(E_+ - E_-)/4t_0L]$ , where  $G_0 = 2e^2/h$  and  $E_{\pm}$  are the ground-state energies of a large auxiliary ring consisting of  $L$  noninteracting sites and an embedded DQD, with periodic and antiperiodic boundary conditions, respectively. The chemical potential is set in the middle of the band, which corresponds to  $L$  electrons in the ring. The method proved to be very efficient for various systems with Kondo correlations.<sup>22,37-39</sup> Up to  $N \sim 5000$  sites were used with a variational ansatz based on  $\sim 100$  projection operators, which was sufficient to obtain converged results for the boundaries between various regimes.

For large interdot tunneling  $t \gtrsim U$  molecular bonding and antibonding orbitals with energies  $\epsilon_{b(a)} = \epsilon \mp t$  are formed. Whenever either of the two orbitals is singly occupied, the physics is analogous to the single impurity Anderson problem with unitary transmission and Kondo correlations (1K regime). When the bonding orbital is doubly occupied, the electrons form an *orbital spin-singlet* (OSS) state with diminished conductance as the Kondo peak in the density of states is absent. The other limit,  $t \rightarrow 0$ , is more interesting. When interdot repulsion is also moderate  $V \lesssim U$ , the dots are effectively decoupled and at the particle-hole symmetric point ( $\epsilon + U/2 + V = 0$ ) the 2K state occurs. Regimes with different occupancies are separated by the intermediate valence regime of width determined by the noninteracting hybridization  $\Gamma = t'^2/t_0$ .

The behavior of the system is less obvious in the intermediate region  $0 \lesssim t \lesssim U$ . In Figs. 1(a)–1(c) we plot the conductance, occupancy, and spin-spin correlation for  $V=0$  and  $U$  ( $\Gamma = t_0/25$  and  $U/\Gamma = 15$  are kept constant throughout the paper). The curves for  $t = \Gamma, V=U$  (dash-dotted thin lines) are the most reminiscent of known results for the single impurity case. The wide plateau in the conductance curve corresponds to the single occupancy regime. While the occupancy for the case with reduced  $t = \Gamma/5$  (dashed thin line) does not change significantly, two maxima in conductance become discernible. One reflects the 1K Kondo physics corresponding to the bonding orbital ( $n=1$  there). The other maximum (with unitary conductance) is known from the  $V=0$  case<sup>16,21</sup> and occurs generally at the transition between the extended Kondo and decoupled spin-singlet states at  $n \sim 2$ . For smaller  $t = \Gamma/50$  at  $n \sim 1$  the conductance is significantly reduced, but the ground state is still 1K, which is signaled by the remaining plateau in occupancy and diminished fluctuations of the occupation of the relevant (i.e., bonding or antibonding) orbital (not shown here). In this case the OSS state is not energetically favorable near  $n \sim 2$ ; correspondingly the conductance peak with the unitary conductance is absent (likewise for  $V=0, t = \Gamma/5$ , where the LSS is not energetically preferred). At  $n=2$  rather the EKT phase is found, as discussed later.

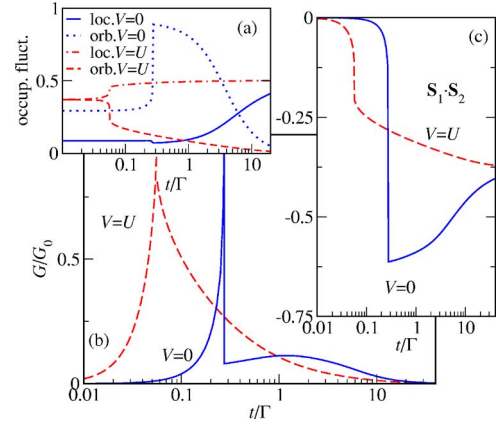


FIG. 2. (Color online) (a) Orbital  $\Delta n_b^2 = \Delta n_a^2$  and site  $\Delta n_1^2 = \Delta n_2^2$  occupancy fluctuations at half filling ( $n=2$ ) as a function of  $t/\Gamma$  for  $V=0$  and  $U$ . Conductance (b) and spin-spin correlation (c), for  $V=0$  (full) and  $U$  (dashed).

The  $V=0$  case is seen to differ qualitatively from the  $V=U$  case. Crude insight into the distinction between the two may be gained from treating just the filling properties of a detached system.<sup>40</sup> The first electron is added when  $\epsilon = t$ , and the second when  $\epsilon = -t + J - [(U+V) - |U-V|]/2$ , where  $J = [-|U-V| + \sqrt{(U-V)^2 + 16t^2}]/2$  is the difference between the singlet and triplet energies of the isolated DQD. When  $n=2$  the ground state is  $[\alpha(|\uparrow\downarrow\rangle - |\downarrow\uparrow\rangle) + \beta(|20\rangle + |02\rangle)]/\sqrt{2}$ , where  $\alpha/\beta = 4t/(V-U + \sqrt{(U-V)^2 + 16t^2})$ . For  $V=0$  and  $U$  the values of  $\epsilon$  where the occupancy of the ground state changes from  $n=0$  to 1 and from  $n=1$  to 2 are indicated by vertical lines on Fig. 1(a). The range of  $\epsilon$  where single occupation is favorable is diminished in the  $V=0$  case.

This observation remains valid also for a DQD attached to the leads, Fig. 1(b). Apparently surprising feature is seen in Fig. 1(c), where the expectation value of the spin-spin correlator  $\mathbf{S}_1 \cdot \mathbf{S}_2$  is seen to approach  $-3/8$  near  $n=2$ , but in fact it is just equal to the noninteracting result with two electrons occupying the bonding orbital. The fact that the spin-spin correlator approaches  $-3/4$  near  $n=2$  in the  $V=0, t = \Gamma$  case suggests that the local picture prevails. The electrons indeed form a singlet in the local basis, which is seen also in the diminished value of the local occupancy fluctuations, Fig. 2(a). Additional insight into the precise role of interdot interaction can be obtained by rewriting the total Hamiltonian in the basis of orbital operators,

$$H_d = \sum_{a=a,b} \left( \epsilon_a n_a + \frac{U+V}{2} (n_{a\uparrow} n_{a\downarrow} + n_{a\uparrow} n_{\bar{a}\downarrow}) \right) + V \sum_{\sigma} n_{a\sigma} n_{b\sigma} + \frac{U-V}{2} (C_{\text{flip}} - S_{\text{flip}}),$$

where the notation  $\bar{a}=b, \bar{b}=a$  is used. The last term of  $H_d$  consists of charge-flip  $C_{\text{flip}} = T_a^+ T_b^- + \text{H.c.}$  and spin-flip  $S_{\text{flip}} = S_a^+ S_b^- + \text{H.c.}$  operators, where  $S_{\lambda}^{\pm} = c_{\lambda\downarrow}^{\dagger} c_{\lambda\uparrow} = (S_{\lambda}^{\pm})^{\dagger}$  are spin and  $T_{\lambda}^{\pm} = c_{\lambda\uparrow}^{\dagger} c_{\lambda\downarrow} = (T_{\lambda}^{\pm})^{\dagger}$  charge<sup>41</sup> (isospin) lowering and raising operators for the orbitals  $\lambda=b, a$  (or sites  $\lambda=1, 2$ ). The full spin

(isospin) algebra is closed with operators  $S_\lambda^z = (n_{\lambda\uparrow} - n_{\lambda\downarrow})/2$  and  $T_\lambda^z = (n_\lambda - 1)/2$ , respectively.

When  $V=U$ , the spin- and isospin-flip terms in  $H_d$  are absent: the Hamiltonian is mapped exactly to the two-level Hamiltonian with intra- and interlevel interaction  $U$  with the bonding and antibonding levels coupled to even and odd transmission channels, respectively. When  $V \neq U$  this mapping is no longer strictly valid. Taking the  $V=0$  case as an extreme example, we find two mechanisms responsible for this. First, the electrons can avoid the interlevel repulsion by occupying aligned spin states in different orbitals, and second, charge-flip terms induce fluctuations of charge between orbitals. Both mechanisms prohibit electrons from occupying well-defined orbital states.

In the rest of the paper we concentrate on the symmetric point of the model,  $n=2$ . Manifestations of the adequacy of the orbital picture are the fluctuations of occupancy  $\Delta n_\lambda^2 = (n_\lambda - \langle n_\lambda \rangle)^2$ , shown in Fig. 2(a). For  $V=U$  orbital occupancy fluctuations  $\Delta n_b^2 (= \Delta n_a^2$  for  $n=2$ ) are indeed smaller than local occupancy fluctuations  $\Delta n_1^2 = \Delta n_2^2$  for all values of  $t$ . On the contrary, for  $V=0$ ,  $\Delta n_b^2 < \Delta n_1^2$  only for  $t \geq 5U$ .

To explain the conductance and spin-spin correlation shown in Figs. 2(b) and 2(c) we first note that the electrons bind into a singlet (local or orbital, depending on  $V/U$ ), whenever  $J \geq J_c = 2.2T_K$ , which is known for the  $V=0$  results,<sup>13,43</sup> but we find that this result can be readily generalized by taking the difference between singlet and triplet energies  $J$  also for  $V>0$ . This relation indicates that although the Kondo temperature is known to rise in the  $V=U$  case<sup>35</sup> for  $n=2$ , the OSS state is energetically favorable for moderate  $t$  as  $J(V \sim U) \propto t$  is larger when compared to  $J(V=0) \sim 4t^2/U$ .

It should be noted that due to the variational nature of the method, the boundaries between various regimes are accurately reproduced. Sharp transitions of correlation functions in the vicinity of crossovers are less precisely determined. The transitions discussed here are actually smoothed into crossovers, which happens generally when parity breaking terms (here the interdot tunneling) are present in the Hamiltonian.<sup>42</sup>

For  $V=0$  in the absence of interdot tunneling  $t \rightarrow 0$ , each of the dots forms a Kondo singlet with its own lead (2K regime). When  $t$  is increased above some value  $t_c$ , set by  $J \geq J_c$ , the ground state becomes a LSS, which is seen from the increased value of  $-\mathbf{S}_1 \cdot \mathbf{S}_2 \rightarrow 3/4$ . The conductance is small in both cases due to the effectively decoupled leads in the 2K case or the deficiency of states near the chemical potential in the LSS case. The conductance  $G \rightarrow G_0$  at some point, which is most vividly understood in terms of the phase shift between odd and even transmission channels, changing from 0 to  $\pi$  during the transition.<sup>16</sup> For  $V \leq U$  the behavior does not change qualitatively, as the transition remains close to  $2T_K \sim J$ . In the case  $V \sim U$  numerical results show deviations from this prediction: the transition occurs at smaller values of  $t$  than set with the relation  $J \geq J_c$ . We explain this by the increased Kondo temperature in the EKT phase as suggested from NRG results.<sup>35</sup> Here the transition between SU(4) Kondo<sup>44</sup> and OSS states occurs at  $T_K^{\text{SU}(4)} \sim J(V=U) = 2t_c^*$ .

On further increasing  $V$  above  $U$  we find that, in contrast

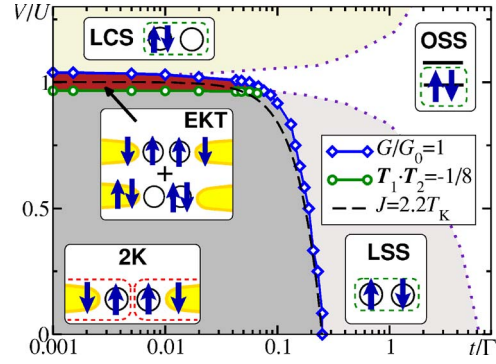


FIG. 3. (Color online) Phase diagram in  $(t/\Gamma, V/U)$  plane for  $n=2$ .

to the strict  $t=0$  case where the ground state for  $V \geq U$  is a non-Fermi-liquid charge-degenerate phase,<sup>35</sup> a finite  $t$  breaks the degeneracy resulting in a (Fermi liquid) phase with increased magnitude of isospin-isospin correlation  $\mathbf{T}_1 \cdot \mathbf{T}_2$ : a *local charge singlet* (LCS). The LCS corresponds to the ground state of a detached system for  $(V-U)/t \gg 1$ .

In Fig. 3 the phase diagram of the DQD for  $n=2$  is shown. The borderline between Kondo and local-singlet phases (full line with diamonds) is characterized by unitary conductance and the abrupt increase of  $-\mathbf{S}_1 \cdot \mathbf{S}_2$  for the transition between 2K and LSS states and of  $-\mathbf{T}_1 \cdot \mathbf{T}_2$  for the transition between EKT and LCS states [see also Figs. 2(a), 2(b), 4(b), and 4(c)]. In the  $t, t' \rightarrow 0$  limit the states  $(2, 0)$   $(0, 2)$  and four states  $(1, 1)$  are degenerate, and  $\langle -\mathbf{T}_1 \cdot \mathbf{T}_2 \rangle < 1/4$ , if the expectation value is taken with respect to these states. We quantitatively characterize the transition to the EKT phase (full line with circles) when  $-\mathbf{T}_1 \cdot \mathbf{T}_2 > 1/8$ . The borderlines that we use to distinguish between local and orbital regimes (dotted) are given by  $\Delta n_b^2 = \Delta n_1^2$  for  $V < U$  and by  $-\mathbf{S}_1 \cdot \mathbf{S}_2 = 3/16$  (half of the noninteracting value) for  $V > U$ .

In Fig. 4 we sample the phase diagram at different  $t$  by increasing  $V$ . We plot three different cases. In the first case (full curve) the DQD is already in the LSS state at  $V=0$ . By increasing  $V$  we see a crossover to a LCS through the orbital

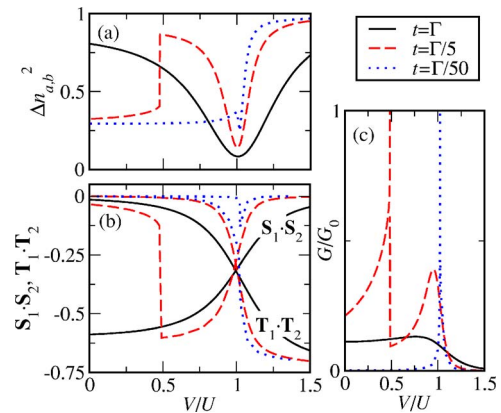


FIG. 4. (Color online) (a) Fluctuations of charge in orbitals  $\Delta n_a^2 = \Delta n_b^2$ . (b) The spin-spin  $\mathbf{S}_1 \cdot \mathbf{S}_2$  and isospin-isospin  $\mathbf{T}_1 \cdot \mathbf{T}_2$  correlations for  $t > t_c$  (full),  $t_c^* < t < t_c$  (dashed), and  $t < t_c^*$  (dotted). (c) The conductance for the three cases.

regime. In the other two cases we start in the 2K phase. Now if  $t < t_c^*$  (dotted) we stay in the Kondo regime until the transition to a LCS happens with the unitary conductance at the transition point. However, if  $t > t_c$  (dashed) there is an area in between where the LSS is energetically favorable. From the point where the system is in a LSS, it follows the same scenario as in the first case.

Finally, let us briefly comment on the  $V > U$  part of the phase diagram. This regime could arise when the dots are capacitively coupled while the on-site repulsion is reduced due to the coupling to local Einstein vibrational modes.<sup>39,45</sup> Here the competition between LCS and EKT phases is relevant for the ground state. Our numerical data confirm NRG predictions that the Kondo regime is relevant only for a small increase of  $V$  over  $U$ . For the parameters used here, we find critical  $V_c \sim U + U/20$ .

In conclusion, we have presented the phase diagram of a pair of tunneling-coupled quantum dots with Coulomb inter- and intradot interactions. In general, the behavior of the  $V \sim U$  case was found to differ from the  $V \sim 0$  case due to the different arrangement of orbital levels of a decoupled system. In addition, for  $V \sim U$  the correct exchange coupling is not  $J \sim 4t^2/U$  but rather  $J \sim 2t$ ; hence the spin-singlet binding energy is increased. The increase in  $J$  is seen to surmount the enhancement of Kondo temperature, which is due to the additional degeneracy in the charge sector. Therefore this enhanced Kondo effect for  $n=2$  should be discernible in measurements only in a tiny window of tunneling rates and interdot vs intradot interaction.

We thank R. Žitko for valuable discussions and acknowledge the support of MSZS under Grant No. PI-0044.

- <sup>1</sup>For a review see, e.g., S. M. Reimann and M. Manninen, *Rev. Mod. Phys.* **74**, 1283 (2002).
- <sup>2</sup>M. Kemerink and L. W. Molenkamp, *Appl. Phys. Lett.* **65**, 1012 (1994).
- <sup>3</sup>R. H. Blick, D. Pfannkuche, R. J. Haug, K. v. Klitzing, and K. Eberl, *Phys. Rev. Lett.* **80**, 4032 (1998).
- <sup>4</sup>W. G. van der Wiel, S. De Franceschi, J. M. Elzerman, T. Fujisawa, S. Tarucha, and L. P. Kouwenhoven, *Rev. Mod. Phys.* **75**, 1 (2003).
- <sup>5</sup>I. Žutić, J. Fabian, and S. Das Sarma, *Rev. Mod. Phys.* **76**, 323 (2004).
- <sup>6</sup>M. A. Nielsen and I. A. Chuang, *Quantum Information and Quantum Computation* (Cambridge University Press, Cambridge, U.K., 2001).
- <sup>7</sup>D. P. DiVincenzo, *Science* **309**, 2173 (2005).
- <sup>8</sup>D. Goldhaber-Gordon, H. Shtrikman, D. Mahalu, D. Abusch Magder, U. Meirav, and M. A. Kastner, *Nature (London)* **391**, 156 (1998).
- <sup>9</sup>H. Jeong, A. M. Chang, and M. R. Melloch, *Science* **293**, 2221 (2001).
- <sup>10</sup>U. Wilhelm, J. Schmid, J. Weis, and K. v. Klitzing, *Physica E (Amsterdam)* **14**, 385 (2002).
- <sup>11</sup>A. W. Holleitner, R. H. Blick, A. K. Hüttel, K. Eberl, and J. P. Kotthaus, *Science* **297**, 70 (2002).
- <sup>12</sup>S. Sasaki, S. Amaha, N. Asakawa, M. Eto, and S. Tarucha, *Phys. Rev. Lett.* **93**, 017205 (2004).
- <sup>13</sup>B. A. Jones, C. M. Varma, and J. W. Wilkins, *Phys. Rev. Lett.* **61**, 125 (1988).
- <sup>14</sup>B. A. Jones and C. M. Varma, *Phys. Rev. B* **40**, 324 (1989).
- <sup>15</sup>T. Aono, M. Eto, and K. Kawamura, *J. Phys. Soc. Jpn.* **67**, 1860 (1998).
- <sup>16</sup>A. Georges and Y. Meir, *Phys. Rev. Lett.* **82**, 3508 (1999).
- <sup>17</sup>R. Aguado and D. C. Langreth, *Phys. Rev. Lett.* **85**, 1946 (2000).
- <sup>18</sup>T. Aono and M. Eto, *Phys. Rev. B* **63**, 125327 (2001).
- <sup>19</sup>R. Lopez, R. Aguado, and G. Platero, *Phys. Rev. Lett.* **89**, 136802 (2002).
- <sup>20</sup>W. Izumida, O. Sakai, and Y. Shimizu, *Physica B* **259-261**, 215 (1999).
- <sup>21</sup>W. Izumida and O. Sakai, *Phys. Rev. B* **62**, 10260 (2000).
- <sup>22</sup>R. Žitko, J. Bonča, A. Ramšak, and T. Rejec, *Phys. Rev. B* **73**, 153307 (2006).
- <sup>23</sup>J. Q. You and H. Z. Zheng, *Phys. Rev. B* **60**, 13314 (1999).
- <sup>24</sup>S. Lamba and S. K. Joshi, *Phys. Rev. B* **62**, 1580 (2000).
- <sup>25</sup>C. A. Büsser, E. V. Anda, A. L. Lima, M. A. Davidovich, and G. Chiappe, *Phys. Rev. B* **62**, 9907 (2000).
- <sup>26</sup>B. R. Buřka and T. Kostyrko, *Phys. Rev. B* **70**, 205333 (2004).
- <sup>27</sup>T. Pohjola, H. Schoeller, and G. Schön, *Europhys. Lett.* **54**, 241 (2001).
- <sup>28</sup>L. Borda, G. Zaránd, W. Hofstetter, B. I. Halperin, and Jan von Delft, *Phys. Rev. Lett.* **90**, 026602 (2003).
- <sup>29</sup>R. Sakano and N. Kawakami, *J. Electron Microsc.* **54** (Supplement 1), 57 (2004).
- <sup>30</sup>R. Sakano and N. Kawakami, *Phys. Rev. B* **72**, 085303 (2005).
- <sup>31</sup>A. L. Chudnovskiy, *Europhys. Lett.* **71**, 672 (2005).
- <sup>32</sup>P. Jarillo-Herrero, J. Kong, H. S. J. van der Zant, C. Dekker, L. P. Kouwenhoven, and S. de Franceschi, *Nature (London)* **434**, 484 (2005).
- <sup>33</sup>Manh-Soo Choi, R. López, and R. Aguado, *Phys. Rev. Lett.* **95**, 067204 (2005).
- <sup>34</sup>O. Yu. Kolesnychenko, R. de Kort, M. I. Katsnelson, A. I. Lichtenstein, and H. van Kempen, *Nature (London)* **415**, 507 (2002).
- <sup>35</sup>M. R. Galpin, D. E. Logan, and H. R. Krishnamurthy, *Phys. Rev. Lett.* **94**, 186406 (2005).
- <sup>36</sup>O. Gunnarsson and K. Schönhammer, *Phys. Rev. B* **31**, 4815 (1985).
- <sup>37</sup>T. Rejec and A. Ramšak, *Phys. Rev. B* **68**, 035342 (2003); **68**, 033306 (2003).
- <sup>38</sup>J. Bonča, A. Ramšak, and T. Rejec, cond-mat/0407590 (unpublished).
- <sup>39</sup>J. Mravlje, A. Ramšak, and T. Rejec, *Phys. Rev. B* **72**, 121403(R) (2005).
- <sup>40</sup>A. B. Harris and R. V. Lange, *Phys. Rev.* **157**, 295 (1967).
- <sup>41</sup>A. Taraphder and P. Coleman, *Phys. Rev. Lett.* **66**, 2814 (1991).
- <sup>42</sup>O. Sakai and Y. Shimizu, *Solid State Commun.* **71**, 81 (1990).
- <sup>43</sup> $T_K = \sqrt{U\Gamma}/2\exp(-\pi U/8\Gamma)$ ; F. D. M. Haldane, *Phys. Rev. Lett.* **40**, 416 (1978).
- <sup>44</sup>The SU(4) Kondo state is seen also in increased value of  $-T_1 \cdot T_2$ , but simultaneously with  $S_1 \cdot S_2 \sim 0$ .
- <sup>45</sup>A. C. Hewson and D. M. News, *J. Phys. C* **13**, 4477 (1980).